Available online at www.sciencedirect.com
SCIENCE DIRECT®
Thin Solid Films 496 (2006) 26 – 29
thin solid films
www.elsevier.com/locate/tsf

Hybrid photovoltaic devices of polymer and ZnO nanofiber composites

Dana C. Olson [b,*], Jorge Piris [a], Reuben T. Collins [b], Sean E. Shaheen [a], David S. Ginley [a]

[a] National Renewable Energy Laboratory, Golden, CO 80401, United States
[b] Department of Physics, Colorado School of Mines, Golden, CO 80401, United States

Available online 15 September 2005

Abstract

Organic semiconductor-based photovoltaic devices offer the promise of a low-cost photovoltaic technology that could be manufactured via large-scale, roll-to-roll printing techniques. Existing organic photovoltaic devices have currently achieved solar power conversion efficiencies greater than 3%. Although encouraging, the reasons higher efficiencies have not been achieved are poor overlap between the absorption spectrum of the organic chromophores and the solar spectrum, non-ideal band alignment between the donor and acceptor species, and low charge carrier mobilities resulting from the disordered nature of organic semiconductors. To address the latter issues, we are investigating the development of nanostructured oxide/conjugated polymer composite photovoltaic (PV) devices. These composites can take advantage of the high electron mobilities attainable in oxide semiconductors and can be fabricated using low-temperature solution-based growth techniques. Additionally, the morphology of the composite can be controlled in a systematic way through control of the nanostructured oxide growth. ZnO nanostructures that are vertically aligned with respect to the substrate have been grown. Here we discuss the fabrication of such nanostructures and present results from ZnO nanofiber/poly(3-hexylthiophene) (P3HT) composite PV devices. The best performance with this cell structure produced an open circuit voltage (V_{oc}) of 440 mV, a short circuit current density (J_{sc}) of 2.2 mA/cm^2, a fill factor (FF) of 0.56, and a conversion efficiency (η) of 0.53%. Incorporation of a blend of P3HT and (6,6)-phenyl C_{61} butyric acid methyl ester (PCBM) into the ZnO nanofibers produced enhanced performance with a V_{oc} of 475 mV, J_{sc} of 10.0 mA/cm^2, FF of 0.43, and η of 2.03%. The power efficiency is limited in these devices by the large fiber spacing and the reduced V_{oc}.
© 2005 Elsevier B.V. All rights reserved.

Keywords: Polymers; Solar cells; Zinc oxide; Nanostructures

1. Introduction

The field of organic-based photovoltaics (OPV) has grown recently due to the potential for a low-cost, large area alternative to conventional photovoltaics. The aim of this research field is to produce PV technology that can be fabricated at low cost using high throughput roll-to-roll processing on flexible substrates. Ideally, all of the steps in the device fabrication would be done using low-temperature solution-based processing that would allow for the use of plastic substrates [1].

Current OPV devices based on composite blends of a π-conjugated polymer, such as poly(3-hexylthiophene) (P3HT) and a soluble form of C_{60} called (6,6)-phenyl C_{61} butyric acid methyl ester (PCBM), have exhibited solar power conversion efficiencies greater than 3% [2]. These devices rely on ultra-fast photoinduced charge transfer between the electron donor P3HT and the acceptor PCBM to dissociate excitons created in the bulk of the film.

Conjugated polymer photovoltaic devices have many positive properties that may provide the means to overcome the current hurdles toward low-cost photovoltaics. However, polymer-based organic PV are presently limited in their power efficiency due to a number of device and material parameters that have yet to be optimized. The first such limitation is that the band gap of the conjugated polymers needs to be decreased in order to absorb a larger portion of the solar spectrum and increase the photocurrent. The photovoltage could be increased by the proper optimization of the band offsets; where the lowest unoccupied molecular orbital of the donor and the valence band of the acceptor are close in energy, but still allow for efficient electron transfer. If the band alignment between donor and acceptor materials was more appropriately engineered through the proper selection and design of active materials, this lost energy could be utilized resulting in

* Corresponding author. Tel.:+1 303 384 6422; fax: +1 303 384 6430.
E-mail address: dana_olson@nrel.gov (D.C. Olson).

0040-6090/$ - see front matter © 2005 Elsevier B.V. All rights reserved.
doi:10.1016/j.tsf.2005.08.179

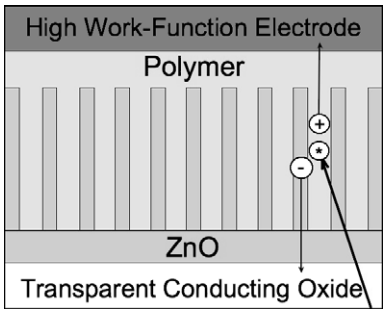

Fig. 1. Schematic diagram of an ideal nanostructured oxide/conjugated polymer photovoltaic device.

improved device performance. Another key factor in OPV device design is the careful control of morphology, leading to efficient dissociation of all generated excitons, and subsequent transport of charge carriers out of the device. Present blend devices rely on morphological control through solvent selection and annealing processes; however, these disordered material structures lead to increased recombination and reduced carrier mobilities and power efficiencies.

Recently, it has been shown that ultra-fast photoinduced charge transfer can also occur between a conjugated polymer and a metal oxide semiconductor such as SnO_2, TiO_2, or ZnO [3]. This has led to the fabrication of PV devices based on composites of oxide semiconductor nanoparticles embedded in a conjugated polymer matrix [4] as well as devices based on infiltrating conjugated polymers into a mesoporous, nanostructured oxide semiconductor network [1,5]. These studies have shown the feasibility of this approach, although the morphology of the nanostructured oxide has not been ideal in these cases, and the device efficiencies have not exceeded 2%.

A promising route to increasing the efficiencies of these devices is to use a nanostructured oxide that is vertically aligned with respect to the substrate such as ZnO nanofibers [6]. This has both the advantages of increasing the donor–acceptor interfacial area and creating electron transport pathways toward the negative electrode that possess very high electron mobility. For instance, the electron mobility of ZnO thin films has been measured as high as 100 $cm^2\ V^{-1}\ s^{-1}$ [7,8], which is several orders of magnitude higher than what is typically found in organic semiconductors. The morphology of the composite is fixed so the donor–acceptor interface does not change, which may lead to better device lifetimes. In addition, metal oxides are currently lower in cost than fullerenes reducing material costs in device fabrication. When compared to a traditional blend device, the direction of current flow is inverted, allowing the use of more stabile high work function counter electrodes. Fig. 1 shows schematically what a composite device based on vertically aligned nanostructures might look like.

2. Experimental

Devices were fabricated on patterned indium tin oxide (ITO)-coated glass substrates that were first cleaned by ultrasonic agitation in acetone, chloroform and isopropanol. A nucleation layer of ZnO was spin-coated onto the ITO, which functions as the transparent negative electrode, using a zinc acetate solution in 2-methoxyethanol [9]. After thermal annealing the zinc acetate film for 5 min at 300 °C in air, the ZnO film is rinsed with deionized water and ethanol. Next, ZnO nanofibers were hydrothermally grown from the nucleation layer in a 1 mM solution of zinc nitrate in deionized water for 20 min at 70 °C [10]. The sample was rinsed again and then dried in air for 10 min at 200 °C. For the ZnO fiber/P3HT device, a 200 nm layer of P3HT is then spin-coated from a 30 mg/ml chloroform solution on top of this structure, followed by another thermal anneal at 200 °C for 1 min under an argon atmosphere. In the case of the ZnO fiber/P3HT:PCBM blend device, a 200 nm layer of P3HT:PCBM (1:1 by weight) is spin-coated from a 40 mg/ml chloroform:chlorobenzene (1:1 by volume) solution. An 80 nm silver top contact was deposited via thermal evaporation through a shadow mask to form the positive back electrode with active areas for each device of 0.1 cm^2. A final thermal anneal is done in the presence of oxygen to oxidize the silver top contact and increase its work function as well as to help oxidize the ZnO.

All electrical measurements were taken in air using a Spectralab XT-10 solar simulator with AM1.5 illumination, UV filter, and intensity, corrected by the spectral mismatch factor, of 100 mW/cm^2. Current–voltage (I–V) measurements taken using a Keithley 238 high current source power meter. External quantum efficiency spectra were estimated using a calibrated Si photodiode, with a spot size smaller than the device area. The scanning electron microscopy (SEM) images were recorded on a JEOL 6320 FE-SEM. Profilometry was done using a Dektak 3 profilometer.

3. Results

3.1. Device fabrication

We have successfully fabricated a device very similar in structure to the one shown schematically in Fig. 1 using ZnO nanofibers, grown on a glass/indium tin oxide (ITO) substrate, intercalated with P3HT. Fig. 2 depicts the ZnO nanofiber structure before and after intercalation with P3HT. As shown, the polymer can be effectively intercalated into the ZnO fiber film thus making a hybrid nanostructured oxide/conjugated polymer composite device.

3.2. Current–voltage characteristics

The photovoltaic performance of the ITO/ZnO fiber/P3HT/Ag device was characterized under simulated AM1.5 illumination and is shown in Fig. 3. The device exhibited an open circuit voltage (V_{oc}) of 440 mV, a short circuit current (J_{sc}) of 2.2 mA/cm^2, a fill-factor (FF) of 0.56, and a power efficiency (η) of 0.53%.

There are several possible reasons why the performance of the device is not better. First, the V_{oc} of the device is less than expected from the effective band gap of the donor–acceptor couple, defined as the difference between the energies of the

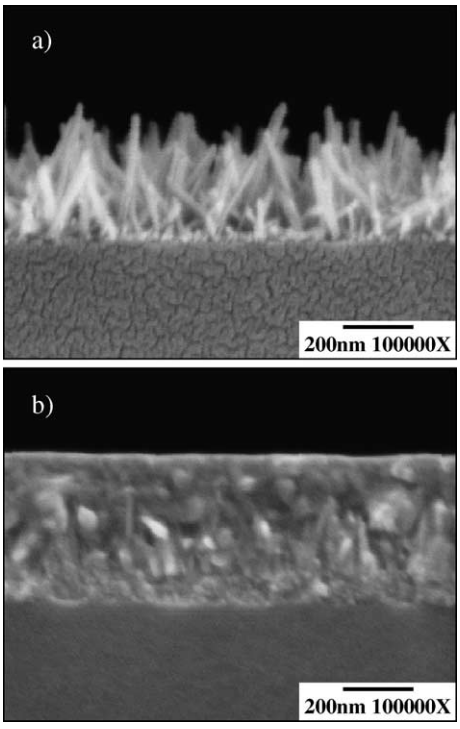

Fig. 2. (a) SEM image of a glass/ZnO nucleation layer/ZnO nanocarpet structure. The ZnO nanofibers are grown from an aqueous solution of zinc nitrate, and the nucleation layer is spin-coated from a zinc acetate solution. (b) SEM image of P3HT intercalated into the nanocarpet structure.

highest occupied molecular orbital (HOMO) of the donor and the lowest unoccupied molecular orbital (LUMO) of the acceptor. In the case of P3HT–ZnO, the effective band gap is approximately 0.9 eV. The reason for the lower measured V_{oc} is not clear, but possible explanations include the presence of mid-gap states on the surface of the ZnO that pin the Fermi level; or the electron mobility of the ZnO nanofibers could actually be too high, resulting in increased carrier recombination at the ZnO/P3HT interface and in a reduced V_{oc}. Further studies are underway to better understand these phenomena.

Secondly, the spacing between the ZnO nanofibers as grown is on the order of 100 nm. This is substantially larger than the typical exciton diffusion length in P3HT, which is presumed to be less than 10 nm, although we do not know how ordering of the P3HT chains inside the pores of the ZnO may affect this. This suggests that closer spacing of the fibers may yield a larger J_{sc}.

In order to dissociate more of the photogenerated excitons in the film and increase the J_{sc} of the cell, a blend of P3HT and PCBM was intercalated into the ZnO nanofiber structure. The resulting device resembles the commonly studied polymer–fullerene device, except that the device structure is again inverted relative to normally fabricated devices and that the ZnO nanofibers are penetrating into the blend morphology. The performance of the ITO/ZnO fiber/P3HT:PCBM/Ag device increased dramatically, demonstrating values for the V_{oc}, J_{sc}, FF and η of 475 mV, 10.0 mA/cm^2, 0.43, and 2.0%, respectively, as seen in Fig. 3. The incorporation of PCBM into the P3HT results in efficient exciton dissociation and nearly a factor of 5 increase in J_{sc} over the device with neat P3HT. This result demonstrates efficient electron transfer from PCBM to ZnO, as there are no direct pathways for electrons to be transferred from PCBM to the underlying ITO without first being transferred to either the ZnO nucleation layer or the ZnO nanofibers. Studies of P3HT:PCBM blends deposited onto planar ZnO nucleation layers grown from zinc acetate precursor (not discussed here) have shown efficient electron transfer from PCBM to this layer. At the moment, we cannot say with certainty that electrons are transferred from PCBM to the ZnO fibers since the fibers and the nucleation layer may have different surface chemistries owing to the different precursors used in their growth. Further studies on this issue are underway. Also, the fill factor of the device is negatively affected upon incorporation of PCBM, which is likely related to the blend morphology not being optimized.

3.3. External quantum efficiency

The external quantum efficiency (EQE) of both the ITO/ZnO fibers/P3HT/Ag and ITO/ZnO fibers/P3HT:PCBM blend/Ag devices are shown in Fig. 4. The ITO/ZnO fibers/P3HT/Ag device shows a maximum EQE of 17.0% at 520 nm, with a clear contribution to the photocurrent from both the P3HT and ZnO counterparts. The peak in the EQE spectrum at about 350 nm results from absorption of ZnO and hole transfer to the P3HT.

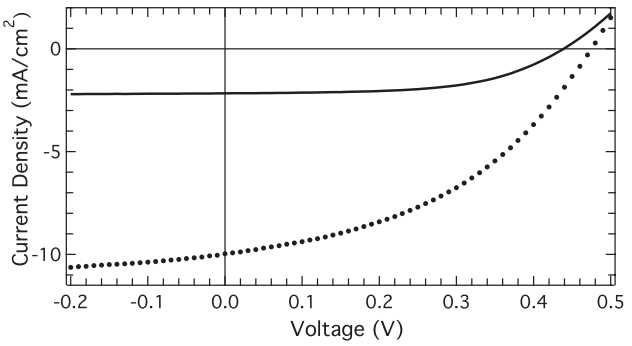

Fig. 3. Current density versus voltage for typical ITO/ZnO fibers/P3HT/Ag device (solid) and ITO/ZnO fibers/P3HT:PCBM blend/Ag device (solid circles) under AM1.5 illumination with an intensity, corrected by the spectral mismatch factor, of 100 mW/cm^2.

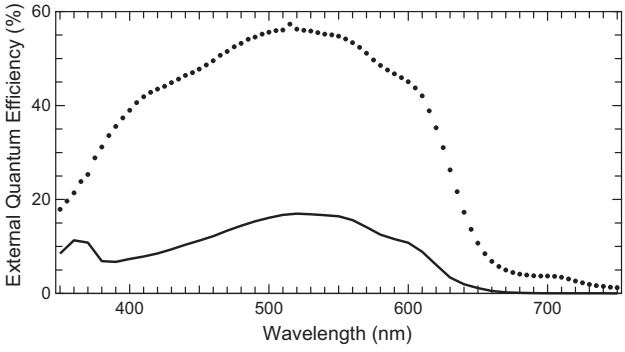

Fig. 4. External quantum efficiency of ITO/ZnO fibers/P3HT/Ag device (solid) and ITO/ZnO fibers/P3HT:PCBM blend/Ag device (solid circles).

When a blend of P3HT:PCBM is added to the nanofibers, a dramatic increase in the EQE is observed to a value over 57% at 515 nm. This increase is likely the result of enhanced exciton dissociation in the film, where the blend effectively reduces the distance between donor and acceptor materials. The absorption and EQE spectrum is broadened over that of the device without PCBM, which is likely due to weak absorption of PCBM in the visible part of the spectrum. This results in increased overlap with the solar spectrum. The EQE spectrum of the ITO/ZnO fiber/P3HT:PCBM blend/Ag device does not show a peak in the UV part of the spectrum from the contribution of the ZnO to the photocurrent, as both the ZnO and PCBM have significant absorption below 360 nm. While there is a significant response in this region, the photocurrent is effectively reduced as the ZnO is acting as a filter for the PCBM/P3HT absorption.

4. Conclusions

In summary, hybrid P3HT/nanostructured oxide devices were fabricated using solution-based methods with efficiencies greater than 0.5%. The P3HT/ZnO device was limited in photocurrent due to the large spacing between the ZnO fibers. This was overcome by blending PCBM into the P3HT film. The enhanced exciton dissociation and efficient electron transfer from PCBM to the ZnO lead to a very high photocurrent and a conversion efficiency in excess of 2% in the blend/ZnO nanofiber device. In order to improve the efficiency in these devices, the fiber spacing must be reduced, thereby increasing the contribution of exciton dissociation by the ZnO fibers. The reason for the reduced V_{oc} must be understood and minimized so as to improve the photovoltage dramatically. To further enhance the photovoltage, the electron affinity could be moved closer to vacuum. All of these steps should lead to improved performance in these devices. Organic PV devices using P3HT:PCBM blends have already demonstrated efficiencies exceeding 3%. The addition of nanostructured transport pathways to the blend may allow for the use of thicker active layers leading to increased efficiencies. The nanostructures may also act to stabilize the morphology of the blend, leading to improved device lifetimes.

Acknowledgements

The authors gratefully acknowledge the many fruitful discussions with Prof. Mike McGehee and Yuxiang Liu at Stanford, Prof. Clark Fields and Rene Peterson at the University of Northern Colorado, and Dr. Brian Gregg and Dr. Garry Rumbles at NREL. The authors also thank Bobby To at NREL for the production of SEM images, Merck for providing P3HT, and financial support for research in organic photovoltaics through the NREL DDRD program and DARPA.

References

[1] S.E. Shaheen, D.S. Ginley, in: Schwarz, Contescu, Putyera (Eds.), Dekker Encyclopedia of Nanoscience and Nanotechnology, Marcel Dekker, Inc., New York, 2004, p. 2879.
[2] F. Padinger, R.S. Rittberger, N.S. Sariciftci, Adv. Funct. Mater. 13 (2003) 85.
[3] P.A. van Hal, M.M. Wienk, J.M. Kroon, W.J.H. Verhees, L.H. Sloof, W.J.H. van Gennip, P. Jonkheijm, R.A.J. Janssen, Adv. Mater. 15 (2003) 118.
[4] W.J.E. Beek, M.M. Wienk, R.A.J. Janssen, Adv. Mater. 16 (2004) 1009.
[5] K.M. Coakley, Y. Liu, M.D. McGehee, K.L. Frindell, G.D. Stucky, Adv. Funct. Mater. 13 (2003) 301.
[6] L. Vaysierres, Adv. Mater. 15 (2003) 464.
[7] R. Könenkamp, L. Dloczik, K. Ernst, C. Olecsh, Physica E 14 (2002) 219.
[8] E.M. Kaidashev, M. Lorenz, H. von Wenckstern, A. Rahm, H.-C. Semmelhack, K.-H. Han, G. Benndorf, C. Bundesmann, H. Hochmuth, M. Grundmann, Appl. Phys. Lett. 82 (2003) 3901.
[9] M. Ohyama, H. Kozuka, T. Yoko, Thin Solid Films 306 (1997) 78.
[10] R.B. Peterson, C.L. Fields, B.A. Gregg, Langmuir 20 (2004) 5114.